# MICROSTRUCTURAL EVOLUTION DURING STECKEL ROLLING AND EBSD ANALYSES OF FINAL MICROSTRUCTURE*

*Altair Lucio de Souza*[1]
*Alisson Paulo de Oliveira*[2]
*Cleiton Arlindo Martins*[3]
*Jacson Morais Borges*[4]
*Joao Junio Pereira Lino*[5]
*Jorge Adam Cleto Cohn*[6]
*Luciano Morais Teixeira*[7]
*Nerea Isasti*[8]
*Beatriz Pereda*[9]
*Pello Uranga*[10]

**Abstract**

A customized version of the Microsim-PM software for one Steckel rolling mill was built and adapted for specific mill parameters. The focus of this study is to use this model, which predicts the austenite grain size distribution evolution during rolling, to understand and quantify metallurgical issues happening during hot rolling. This will allow the steel mill to optimize the rolling process and chemical composition before the first industrial trial. Materials rolled for final thicknesses of 4.75, 6.30 and 12.5 mm of a carbon manganese steel and a microalloyed steel were selected to tailor the equations used by the model and to accurately reproduce the reality of the Steckel mill. This paper analyses the results from the customized model and compares them to mill data and final microstructure. Measured and predicted Mean Flow Stress (MFS) values are compared. After rolling, the material is subjected to accelerated cooling using laminar cooling. These cooling curves obtained from mill data are also considered to analyze the final microstructure characterized for all the cases using EBSD. The quantification of the microstructure allows for a better understanding of the relationship between chemical composition, process parameters and mechanical properties.

**Keywords:** Modelling; EBSD; Microstructure, Mean Flow Stress.

1 *Metallurgist Engineer, Master in Metallurgical and Mining Engineer, Rolling Mill Senior Specialist, Steckel Mill, Gerdau, Ouro Branco-MG, Brasil;*
2 *Metallurgist Engineer, Master in Metallurgical and Mining Engineer, Doctorate student in Metallurgical, Materials and Mining Engineering, Senior Technical Specialist, Steckel Mill R&D, Gerdau, Ouro Branco-MG, Brasil;*
3 *Education/degree, function, section/department, Institution of work or study, city, state, country.*
4 *Production Engineer, Rolling Mill Senior Specialist, Steckel Mill, Gerdau, Ouro Branco-MG, Brasil.*
5 *Metallurgist Engineer, Master in Metallurgical and Mining Engineer, Rolling Mill Senior Specialist, Steckel Mill, Gerdau, Ouro Branco-MG, Brasil.*
6 *MSc, Metallurgical Engineer,, Technical Manager, Steckel Mill R&D, Gerdau, Ouro Branco-MG, Brasil.*
7 *Electronic and Telecommunication Engineer, Automation Specialist, Steckel Mill, Gerdau, Ouro Branco-MG, Brasil.*
8 *PhD, Researcher, Materials and Manufacturing Division, CEIT and Universidad de Navarra, San Sebastian, Basque Country, Spain*
9 *PhD, Researcher, Materials and Manufacturing Division, CEIT and Universidad de Navarra, San Sebastian, Basque Country, Spain*
10 *PhD, Associate Director of Division, Materials and Manufacturing Division, CEIT and Universidad de Navarra, San Sebastian, Basque Country, Spain*

## 1 INTRODUCTION

The balance between chemical composition, mechanical performance and cost effectivity is always a vital point for the development of microalloyed structural steels in hot strip production. A properly developed practical model can be a tool for the process engineer to optimize the alloy/processing design to achieve maximum productivity at the lowest overall costs while still maintaining stable metallurgy/mechanical properties. Based on the MicroSim software, a customized version for a Steckel mill is developed and applied to production. This paper describes the metallurgical logic of the model and gives actual industrial Steckel mill applications to use it for improved metallurgy and costs.

In the current frame, several low carbon CMn and Nb-microalloyed HSLA structural steels were selected and industrially processed. In addition to the conventional information provided by mean grain size evolution models, where a reduction in the final average grain size can be predicted due to the lower rolling temperatures, the output from MicroSim modeling offers the possibility for the prediction of homogeneity enhancement, analyzing the resulting grain size distribution predictions. Once the rolling parameters such as soaking temperature, reduction and temperature strategies are defined, the Mean Flow Stress (MFS) tool allows for the validation of the model comparing measured stresses during rolling (based on roll load measurements) and the model calculations based on microstructural evolution.

MicroSim modeling is limited to the austenite evolution during rolling. Therefore, the microstructural analysis in final products is important to understand the relationship between the austenite after rolling and the microstructure after coiling. The combination of both results helps identifying which type of metallurgical mechanisms are in-play resulting in higher strengths.

## 2 MODEL STRUCTURE and EXPERIMENTAL TECHNIQUES

Mathematical modeling is a useful tool to design hot rolling schedules. Each model has to be built upon the suitable initial hypotheses and boundary conditions. For most application, microstructural modeling evolution can be successfully performed using conventional average grain size evolution models. For most challenging requirements, such as toughness improvement, microstructural homogeneity quantifications are needed as average values are not enough for accurate predictions. In order to overcome this limitation, a model incorporating initial austenite grain size distributions was developed at CEIT [1]. This modeling was initially designed, validated and applied to Thin Slab Direct Rolling plants. Then, this model was transferred to a user-friendly environment, called MicroSim® software, and currently is being expanded to more conventional rolling layouts such as Hot Strip [2] and Plate [3] mill customized facilities.

The model takes as an input the initial austenite grain size distribution and provides the size distributions for recrystallized and unrecrystallized fractions at the entrance of any rolling pass, considering the simultaneous interaction of the mechanisms acting during the interpass time, such as, static and metadynamic recrystallization, grain growth and Nb(C,N) strain induced precipitation. All the equations used were derived for CMn and microalloyed steels, and adapted for a wide range of initial grain sizes. During the last years, additional improvements were added to the model, such as new solubility equations in order to predict the amount of Nb in solution after the reheating furnace. These equations were derived by regression fitting of the solubility curves calculated using Thermocalc (TCFE8 database) software. Also, and based on specific grain growth laboratory tests performed with Nb and Nb-

Ti microalloyed steels, new grain growth equations were fitted.

Based on the calculations, the model analyzes the complete austenite grain size distributions from pass to pass during the hot working process and it supplies the following data:

- Recrystallized fraction.
- Non-recrystallized fraction detailing if the origin is solute drag or strain induced precipitation.
- Mean austenite grain size (Dmean).
- Critical grain size, Dc(0.1). This parameter corresponds to the grain size relative to the 10% of the coarsest grains in the tail of the distribution.
- Maximum austenite grain size (Dmax).
- ZD, the Dmax/Dmean ratio.
- Retained strain.

The application of the model to a specific industrial plant results a valuable tool in the alloy/process design but it can require some level of customization. The present model and related software, MicroSim-Steckel Mill, seeks to provide answers for specific needs of the Steckel Mill at Gerdau Ouro Branco. For this specific development and customization several grades, mainly CMn and Nb microalloyed steels with Ti and V additions in some cases. In this case, especial attention was paid to dynamic recrystallization onset and its effect on Mean Flow Stress (MFS) predictions. The approach developed by Minami et al. [4] was followed for MFS prediction.

Figure 1 shows a screenshot corresponding to the input data screen for a conventional hot strip rolling schedule to produce a 6.3 mm thick strip. The input data screen offers possibilities for detailing the chemical composition, grain size distribution resulting after the preheating furnace with its predefined furnace temperature, number of mill passes for both roughing and finishing stands, as well as all the rolling schedule parameters. Additional capabilities such as creating a result report or loading and saving data are also incorporated.

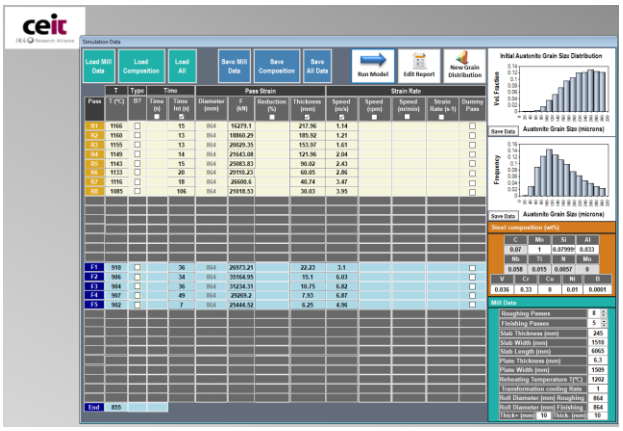

**Figure 1.** Screenshot showing the input data layout for MicroSim-Steckel Mill model.

Figure 2 shows a screenshot of the results displayed when MicroSim is run. Together with plots showing recrystallized fraction evolution and grain size evolution during rolling, a complete table of values is presented. This information is completed with the whole set of grain size distributions plotted in Figure 3. This histograms plot not only the grain size distributions but also the type of austenite grains composing them. That is, in blue the recrystallized grains, in red the non-recrystallized due to strain induced precipitation and in some cases in yellow the non-recrystallized grains due to solute drag.

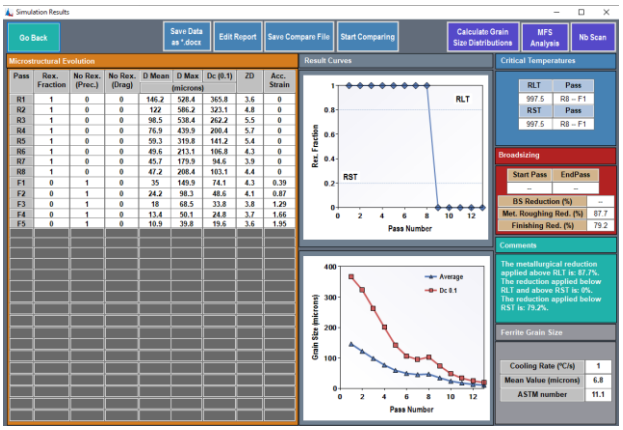

**Figure 2.** Screenshot showing the results for MicroSim-Steckel Mill model.

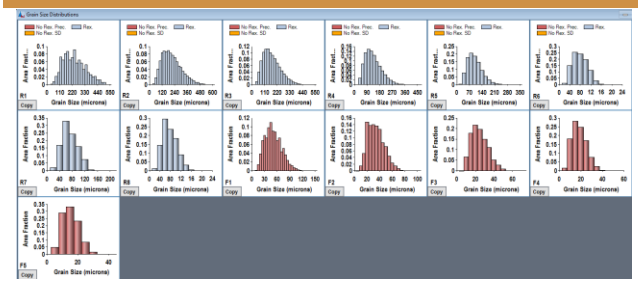

**Figure 3.** Screenshot showing the grain size distribution predictions after each pass for MicroSim-Steckel Mill model.

An additional feature of the MicroSim software is the MFS Analysis tool (see Figure 4). This tool allows for the comparison between the measured MFS values and the calculated ones in the model. This is a convenient way to validate the model predictions. The blue dots in the upper left plot are the measured MFS values (based on the rolling loads) and the yellow dots are the calculated ones. The change in the slope from the roughing passes (at high temperatures) and the finishing passes (at lower temperatures) shows the positive effect of Nb for strain accumulation. In addition to the combined effect of Ti and Nb controlling grain growth during roughing, the austenite pancaking provides an additional mechanism for microstructural refinement during transformation. As shown in the screenshot, the MFS analysis tool also provides information about the reduction strategy followed during rolling and other critical temperatures.

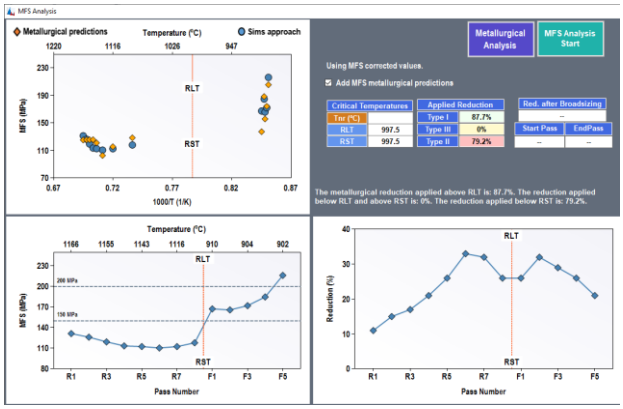


**Figure 4.** Screenshot showing the MFS analysis and the comparison between measured and predicted MFS values for the MicroSim-Steckel Mill model.

The austenite evolution modeling was completed by a complete microstructural characterization of final product samples. The microstructures were characterized by optical microscopy and Field-Emission Gun Scanning Electron Microscopy (FEG-SEM). Electron Backscattered Diffraction (EBSD) scans were performed to quantify the crystallographic features intervening in the mechanical behavior. For this purpose, the samples were polished to 1 μm followed by a finishing with colloidal silica. Orientation imaging microscopy was carried out on the Philips XL30CP SEM with W-filament, using TSL equipment. The selected scan step was 0.6 μm for general microstructure characterization and unit size measurements. The total scanned area was about 200x200 $\mu m^2$. The criteria of 4º and 15º crystallographic misorientation boundaries were selected to quantify the mean grain sizes (Dmean-4º and Dmean-15º) and the corresponding size distributions. The effective grain size was calculated as the equivalent circle diameter related to the individual grain area. The 4º misorientation was selected as these boundaries intervene in the definition of yield strength, while the 15º boundaries are relevant to control brittle crack propagation. Kernel Average Misorientation maps were also obtained in order to evaluate the dislocation densities.

## 3 RESULTS AND DISCUSSION

### 3.1 Austenite Evolution Modeling

As it was shown in Figures 1 to 4, the amount of results coming out from MicroSim simulations is quite important and therefore, comparison between different rolling cases becomes complex. In order to partially overcome this barrier, a tool called MicroSim-Compare was developed. This tool allows for a simple comparison between the most relevant parameters in the simulations. The following Figure 5 summarizes the microstructural evolution during rolling.

Figure 5a shows the evolution of recrystallized fraction from pass to pass. The differences between CMn and Nb steels are very important. In CMn steels most of the passes are applied in a complete recrystallization regime. Partial recrystallization is only achieved after the last finishing pass. For NbTiV steels though, the transition between full recrystallization and full strain accumulation happens in the roughing to finishing transition. This reflects an optimized rolling sequence design for these steel grades. Microstructure would be recrystallized and homogenized several cycles during roughing and the finishing steps will be applied for the austenite conditioning promoted by Nb addition.

Figures 5b and c show the grain size evolution during rolling. Figure 5b shows the progressive reduction in the mean austenite grain size. In this graph too two different families can be noted based on their chemical composition. CMn steels show a gradual decrease with a more erratic behavior during last finishing passes. The differences in the final average grain size are directly related to the rolling finish temperature and total reduction applied. The average grain size reduction in the NbTiV grades is steeper and lasts longer until the end of the rolling. This stronger refinement is a combination of slower recrystallization kinetics due to Nb, reducing time for possible grain growth, and growth hindering due to the combined effect of Nb and Ti. In this case, the final average grain is mostly related to the total reduction as pancaking takes an important role during finishing passes.

The critical grain size parameter (Dc) plotted in Figure 5c reflects the homogeneity of the grain size distribution. Dc or Dc10% is referred to the grain size for which there are 10% of grains bigger than that one. It reflect the extension of the tail of the distribution. The trends in these cases are quite similar to the ones followed by the average grain size. Therefore, it reflects that the progression from pass to

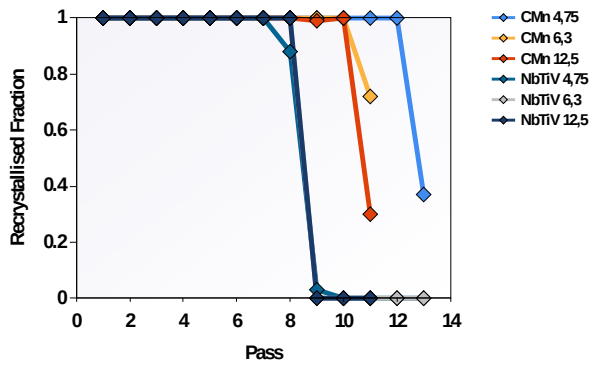


(a)

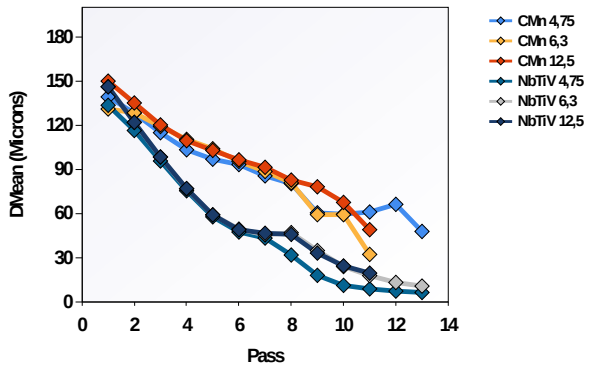


(b)

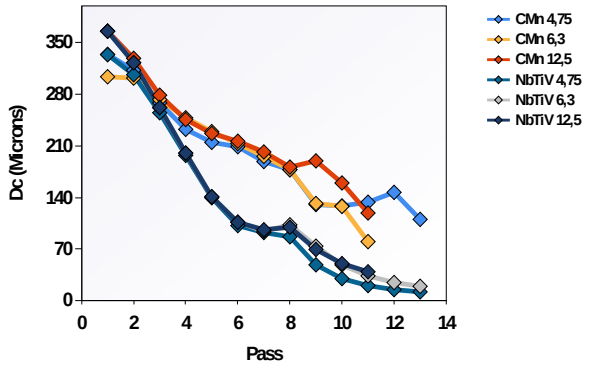


(c)

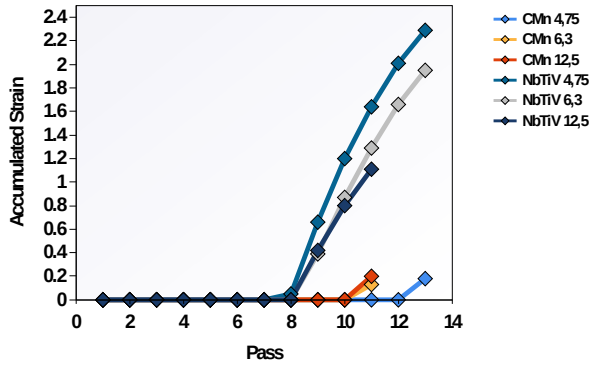


(d)

**Figure 5**. Comparison between austenite evolution calculations for all the cases. (a) Recrystallized fraction (b) Average austenite grain size (Dmean) (c) Critical austenite grain size (Dc) (d) Accumulated Strain evolution

pass is controlled by continuous recrystallization and grain growth. It is worth noting that the lack of continuous recrystallization during roughing and/or incomplete recrystallization during finishing passes might result in a more heterogeneous distribution of grains in austenite. This heterogeneity would be then transferred to final microstructure resulting in a more heterogeneous ferrite distribution or in the presence of coarse bainitic phases transformed from the coarsest austenite grains instead of ferrite.

Finally, Figure 5d shows the comparison between the different trends on the strain accumulation (or austenite pancaking). Again, in this case, the behavior between the CMn steels and NbTiV ones is very clear. The effect that Nb(C,N) strain induced precipitates have on the austenite pancaking during the finishing stands is clear for the three selected thicknesses. The degree of accumulated strain is directly proportional in this case to the reduction applied during finishing, that is, inversely proportional to final thickness.

The combination of fine and homogeneous austenite microstructure with a high degree of accumulated strain will result in a fine and homogeneous final microstructure for a given cooling and coiling strategy after rolling.

### 3.2 Final Microstructure

In Figure 6 and 7 two examples from the 6.3 mm final thickness and both steel grades are shown. As a first step, a general through thickness characterization was performed by optical microscopy detecting the differences between surface, ¼ and centerline areas. In these Figures both micrographs correspond to the ¼ position and were taken in the rolling direction.

The effect of chemical composition is clear from the figures. CMn steels show a more irregular microstructures composed of ferrite grains and some bainitic or acicular areas. Nearby the surface the microstructure is more ferritic and finer and the acicular phases become more predominant near the centerline. This facts reveals some degree of through-thickness heterogeneity. These differences are more relevant for the thicker gauges, i.e. lower total reductions.

In the NbTiV steels though, the microstructure is composed of very fine ferrite grains with some pearlite. The microstructure is more homogeneous both locally and through thickness and shows some elongated directionality inherited from the pancaked austenite. Differences are less evident for different final thicknesses too.

In addition to general microstructural characterization by means of optical microscopy, crystallographic analysis using EBSD was performed. In Figures 6b and Figure 7b two grain boundary maps are shown for the selected different microstructures. The boundaries located between $4º<\vartheta<15º$ (in red) and $\vartheta>15º$ (in black) are considered as low and high angle boundaries, respectively [5]. Low angle misorientation grains are assumed to contribute to strength properties due to their opposition to dislocation movement, whilst high angle boundaries are considered effective for controlling crack propagation.

Regarding the effect chemical composition the modification of microstructural is conveniently addressed by means of EBSD analysis. For the CMn steel a coarse distribution of high angle boundary is noticed. Grains show irregular shapes and the presence of low angle boundaries (red lines) is higher. This factor helps differentiating the ferrite grains from acicular phases. NbTiV steels, on the other hand, show equiaxed fine high angle boundary units, regular and homogeneously distributed. The presence of low angle boundaries is limited, showing that the matrix is formed by ferrite and that acicular/bainitic phases are not formed.

Besides grain boundary structure, EBSD helps estimating the dislocation density

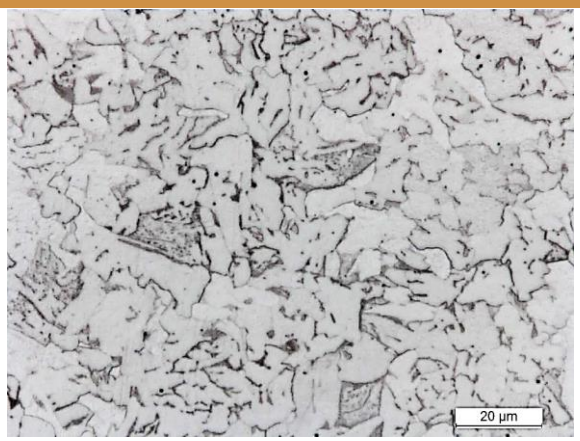


(a)

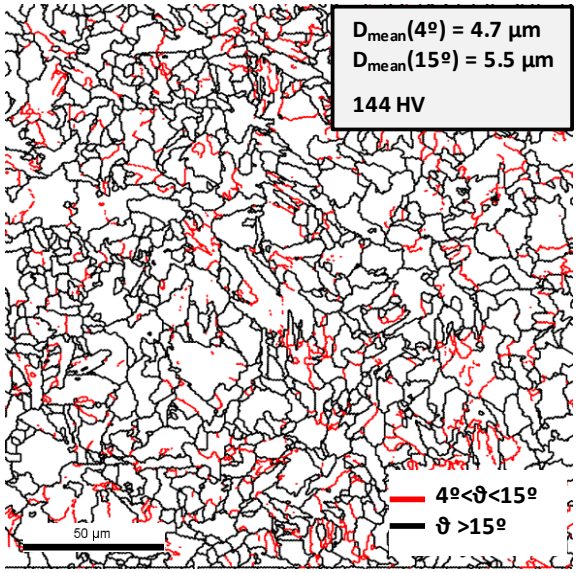


(b)

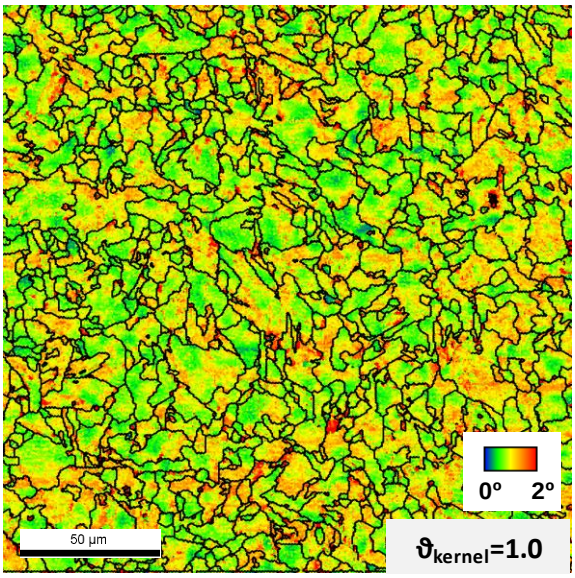


(c)

**Figure 6.** Final microstructure in the CMn steel for a final thickness of 6.3mm and ¼ position. a) Optical micrograph b) EBSD Grain boundary map c) Kernel Average Misorientation map.

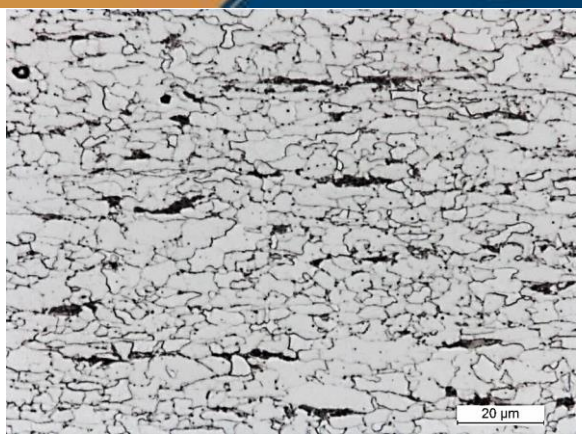


(a)

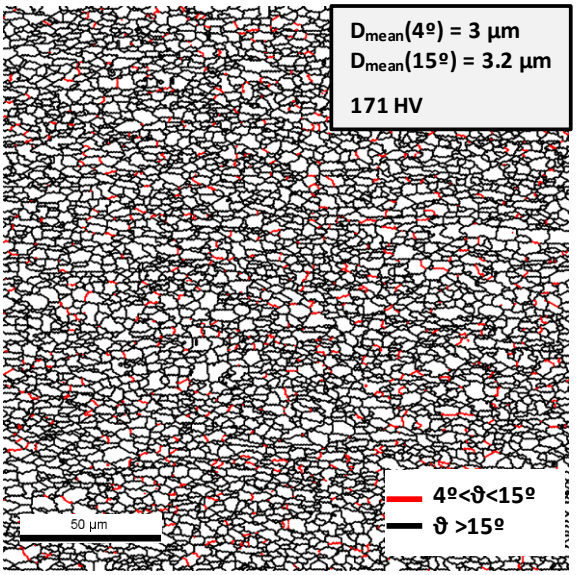


(b)

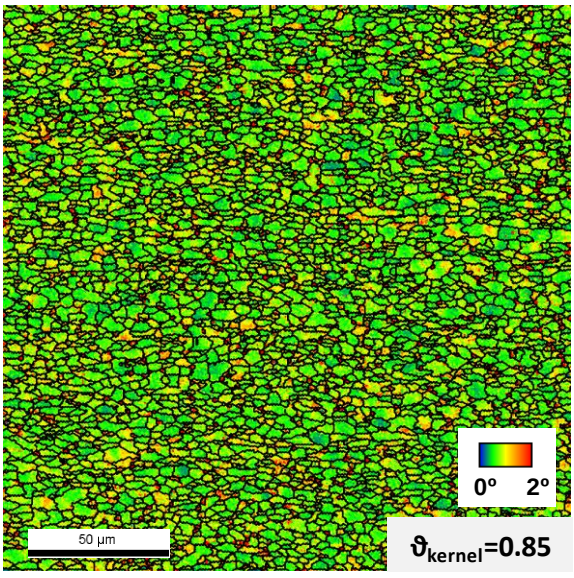


(c)

**Figure 7.** Final microstructure in the NbTiV steel for a final thickness of 6.3mm and ¼ position. a) Optical micrograph b) EBSD Grain boundary map c) Kernel Average Misorientation map.

values by the measurement of local misorientation gradients [6]. For this purpose Kernel Average Misorientation (KAM) parameters are calculated. KAM maps are plotted in Figures 6c and 7c for the CMn and NbTiV steels, respectively. Kernel for local misorientation smaller than 2º and second neighbor criteria were taken into account. In order to minimize the frequent overestimation of the KAM measured using conventional EBSD, the measurements were corrected considering a correlation between high-resolution EBSD and conventional EBSD [7]. The color maps shown in the Figures 6c and 7c clearly show the different level of dislocation densities in both grades. For CMn grade the colors are mostly in the green-orange range denoting a medium-high dislocation density, characteristic of a mostly acicular/bainitic structure. NbTiV steels, meanwhile show predominantly greenish colors, this is also reflected in a lower average KAM value. This characteristic is shown by purely ferritic structures.

In addition to comparison for average grain sizes and dislocation densities, EBSD measurements allow for the quantification of low and high angle unit distributions. The quantification of grain size distributions helps understanding the degree of microstructural homogeneity. For applications where toughness is critical, microstructural homogeneity is a magnitude that must be measured together with average grain sizes [8]. Figure 8 plots the grain size distribution of the six coils analyzed for both low angle boundaries (Figure 8a) and high angle boundary units (Figure 8b). Trends are quite similar in both cases. CMn steels show wider grain size distributions, especially for the thickest final gauge thicknesses. The CMn steel with the 4.75 mm final thickness shows a grain size distribution which is quite close to the one measured in the NbTiV steels. These are the ones with the finest and more homogeneous grain size distributions, both for low and high angle boundary units.

In order to achieve an idea about the degree of homogeneity and the possible impact on toughness properties the values for high angle boundary average and critical (Dc20%) are listed in Table 1. The ratio between the critical and mean grain size is also calculated.

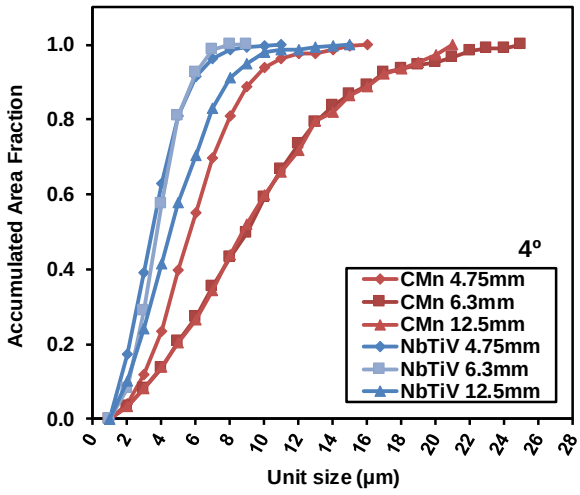


(a)

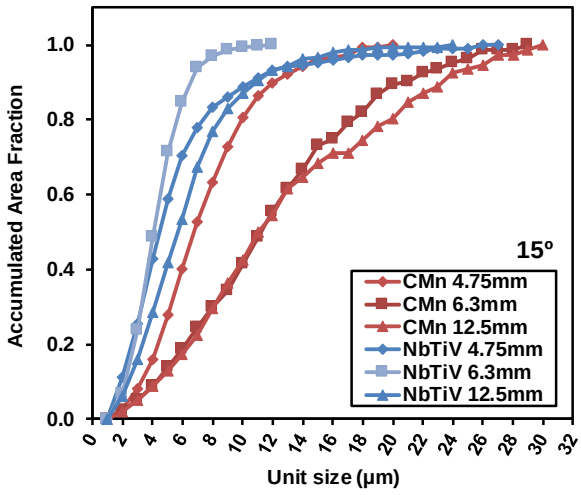


(b)

**Figure 8**. Accumulated grain size distributions for final microstructure and all the samples (a) Low angle boundary units sizes (b) High angle boundary unit sizes.

From the data in Table 1 and the curves in Figure 8, it is clear that for high angle boundary units, the NbTiV steel with a final thickness of 6.3mm is the one showing the finest and most homogeneous microstructure. Combining predictions for austenite grain size distributions from MicroSim with the corresponding coiling temperature (higher coiling temperature in

this case), a perfect balance between a good austenite conditioning and formation of mostly ferritic matrix is achieved. For the other thicknesses of 4.75 and 12.5 mm, the resulting microstructure is more acicular, mainly due to lower coiling temperatures and this is the main reason for the more heterogeneous final distribution.

**Table 1.** Microstructural characterization values measured in final product in order to evaluate the degree of homogeneity

| Sample | D15º (μm) | Dc20% (μm) | Dc20%/D15º |
|---|---|---|---|
| **CMn 4.75mm** | 4.6 | 10 | 2.2 |
| **CMn 6.3mm** | 5.5 | 17.3 | 3.1 |
| **CMn 12.5mm** | 5.6 | 20 | 3.6 |
| **NbTiV 4.75mm** | 3 | 7.5 | 2.5 |
| **NbTiV 6.3mm** | 3.2 | 5.6 | 1.8 |
| **NbTiV 12.5mm** | 3.7 | 8.5 | 2.3 |

### 3.3 Relationship between microstructure and mechanical properties

The yield strength of low carbon microalloyed steels can be calculated as a combination of different strengthening contributions. In this case, a linear approach based on the sum of the contributions (solid solution, grain size, dislocations and fine precipitation) has been considered. The microstructural quantification described in Section 3.2 is the base for the grain size and dislocation density contributions. Due to the lack of an accurate measurements of precipitate volume fractions, the contribution of fine precipitation ($\sigma_{ppt}$) was estimated by subtracting the strengthening associated with all the other contributions from the experimental yield strength. A more detailed description of the expressions used for this quantification can be found in Ref. 5.

In Figure 9 the effect of the different strengthening mechanisms are plotted for all the samples and the calculated values are compared to experimental ones. The results shown in Figure 9 suggest that the most relevant strengthening mechanism is associated with grain size refinement in all the conditions, being this effect stronger for the NbTiV grades.

In CMn steels, the correlation between the calculated contributions and the measured mechanical properties shows some overestimation for the calculated properties, especially for the 4.75 mm thickness.

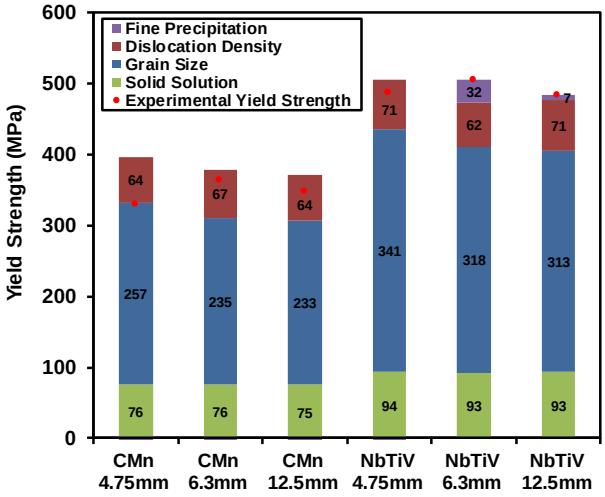


**Figure 9**. Analysis of the strengthening mechanisms acting for the different grades and final thicknesses.

For microalloyed grades, the calculations fit better even if the contribution left for the precipitation strengthening is quite limited. Based on these facts, there could be a possibility for some degree of overestimation on the microstructural refinement and/or dislocation density strengthening. In that case, the contribution of precipitation would become more important in these grades. Anyway, the microstructural refinement is very important for these microalloyed grades and its increase in the final balance should be determining.

Based on the whole set of modeling and characterization results, it can be concluded that the appropriate design of the rolling process together with a convenient chemical composition and the

control of the cooling/coiling strategy would ensure the mechanical properties of final products.

## 4 CONCLUSIONS

MicroSim model was successfully customized for the Gerdau Ouro Branco Steckel mill and we are now working in some fine adjustments. The austenite microstructural simulations show a very effective austenite conditioning in the NbTiV microalloyed steels. Fine and homogeneous austenitic structures are achieved in those grades after the last rolling pass. This homogeneous austenite combined with high retained strains, i.e. pancaked austenite lead to a fine and homogeneous ferritic structure after coiling. The microstructural characterization suggests that the addition of microalloying elements promotes the formation of considerably finer and homogeneous microstructures. More bainitic and coarser microstructures are noticed in the CMn samples mainly due to the lack of austenite conditioning.

Crystallographic characterization by means of EBSD confirms that the addition of Nb ensures an important microstructural refinement. Considerably lower mean unit sizes (considering both misorientation criteria) are measured for the plates containing Nb compared to CMn plates. This increased refinement and more homogeneous structures are measured in terms of the ratio between Dc20% and D15º.

Finally, strengthening individual contributions (solid solution, grain size, dislocation density and fine precipitation) of each hardening mechanism have been estimated for all the cases. The results suggest that the most predominant strengthening mechanism is related to grain size in all the grades.

## Acknowledgments

The authors would like to gratefully acknowledge Companhia Brasileira de Metalurgia e Mineração (CBMM) for funding this project. Authors would lalso like to thank Mr. Marcelo A. Rebellato for his contribution.

## REFERENCES

1 Uranga P, Fernández AI, López B, Rodriguez-Ibabe JM. Modeling of Austenite Grain Size Distribution in Nb Microalloyed Steels Processed by Thin Slab Casting and Direct Rolling (TSDR) Route. ISIJ Int. 2004:44:1416-1425.

2 Uranga P, Rodriguez-Ibabe JM, Stalheim DG, Barbosa R, Rebellato M. Application of Practical Modeling of Microalloyed Steels for Improved Metallurgy, Productivity and Cost Reduction in Hot Strip Mill Applications, Procs AISTech 2016 Conf, 2016:1769-1778.

3 Azpeitia X, Isasti N, Uranga P, Rodriguez Ibabe JM, Stalheim DG, Rebellato M. Through-Thickness Microstructural Optimization in Plate Rolling of Nb-Microalloyed Steels, Procs. 2nd Intl Symp Recent Developments in Plate Steels, 2018:83-91.

4 Minami K, Siciliano F, Maccagno TM, Jonas JJ. Mathematical Modeling of Mean Flow Stress during the Hot Strip Rolling of Nb Steels, ISIJ Int. 1996:36:1507-1515.

5 Larzabal G, Isasti N, Rodriguez-Ibabe JM, Uranga P. Evaluating Strengthening and Impact Toughness Mechanisms for Ferritic and Bainitic Microstructures in Nb, Nb-Mo and Ti-Mo Microalloyed Steels. Metals:2017:7:65.

6 Kubin LP, Mortensen A. Geometrically necessary dislocations and strain-gradient plasticity: a few critical issues. Scripta Mater. 2003:48:119-125.

7 Isasti N, Jorge-Badiola D, Alkorta J, Uranga P. Analysis of Complex Steel Microstructures by High-Resolution EBSD. JOM. 2016:68:215-223.

8 Isasti N, Jorge-Badiola D, Taheri ML, Uranga P. Microstructural Features Controlling Mechanical Properties in Nb-Mo Microalloyed Steels. Part II: Impact Toughness. Met Mat Trans A. 2014:45:4972-4982..